LA-UR-14-20314
Approved for public release; distribution is unlimited.

Title: Post-Cure Studies on Solid Silicone Elastomer: DC745U

Author(s): Ortiz-Acosta, Denisse
Janicke, Michael T.
Yoder, Jacob
Cady, Carl M.

Intended for: Report

Issued: 2014-01-17

Weapon Systems
Engineering Division

# Post-Cure Studies on Solid Silicone Elastomer: DC745U

| Number | Revision | Effective Date |
|---|---|---|
| W-15-TR-0002U | A | 1/15/2014 |

| Approved by | Name | Title/Org | Signature | Date |
|---|---|---|---|---|
| *Authors* | Denisse Ortiz-Acosta | C-CDE |  | 12/05/2013 |
| | Michael Janicke | C-IIAC |  | 12/04/2013 |
| | Jacob Yoder | P-21 | 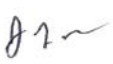 | 12/05/2013 |
| | Carl Cady | MST-8 | 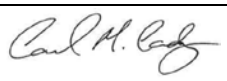 | 12/04/2013 |
| *Reviewer* | Jennifer Gallegos | R&D Engineer/ W-15 | 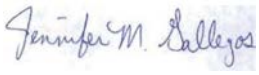 | 12/05/2013 |
| *Group Leader* | Patti Buntain | R&D Manager/ W-15 | 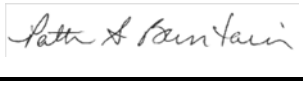 | 1/15/2014 |

| **Status:** | **Comments:** |
|---|---|
| ☑ New<br>☐ Major Revision<br>☐ Minor Revision<br>☐ Reviewed, No Change | |

This document has been deemed
**UNCLASSIFIED** by:
Jennifer Gallegos, R&D Engineer, W-15

## REVISION LOG

| Document Number | Revision | Description of Change |
|---|---|---|
| W-15-TR-0002U | A | Initial release |

## MISSION STATEMENT

As part of the Enhanced Surveillance mission, our goal is to provide suitable lifetime assessment of stockpile materials. This report is an accumulation of new experimental data on the DC745U material and their findings. Our intention is that the B61 Life Extension Program (LEP) use this collection of data to further develop the understanding and potential areas of study.

## ACKNOWLEDGMENTS

Tom Zocco- Enhanced Surveillance Campaign (C8) Program Manager

# TABLE OF CONTENTS

# LIST OF FIGURES



# LIST OF TABLES

## 1.0 INTRODUCTION

DC745U is a silicone elastomer originally manufactured by Dow Corning under the name of Silastic® DC745U at their manufacturing facility in Kendaville, Indiana. Currently DC745U is available through Xiameter® or Dow Corning's distributor R. D. Abbott Company. This silicone elastomer is used in numerous parts of weapon systems, including outer pressure pads, aft cap support in W80 and pressure pad in the B61.

DC745U is a proprietary formulation and limited information about its composition and properties is provided to the customer. Thus, Los Alamos National Laboratory and Lawrence Livermore National Laboratory have performed a variety of characterization experiments on this material.[1-3] Based on NMR studies it was estimated that DC745U is composed of ~ 98.5% dimethyl repeat units, ~ 1.5% methyl-phenyl repeat units, and < 1% of vinyl-methyl siloxane repeat units, as shown in Figure 1. The polymer is filled with ~ 38 wt. % of a mixture of fumed silica and quartz. Additionally, DC745U is cured using a vinyl-specific peroxide initiator known as Varox DBPH-50, Luperox 101, or 2,5-dimethyl-2,5-di(tert-butylperoxy) hexane, manufactured by R.T. Vanderbilt Company. During the curing of the silicone polymer, new crosslinked sites are induced generating a polymer network structure. Formulation, curing conditions, heterogeneities within the material, and production processes will determine the crosslink density and structure of the polymer network, and thus the mechanical, thermal, and physical properties of the final product. (For more information on historical data on DC745U and production process please review the reports by *Denisse Ortiz-Acosta W-1-TR-0098U* and *LA-UR-12-23948*.[3,4])

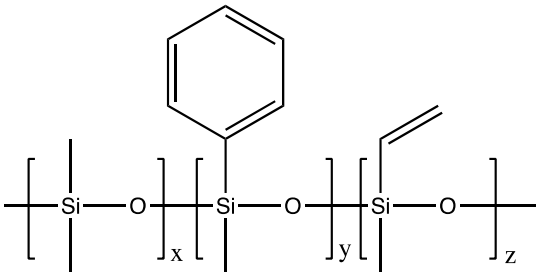


| LLNL | LANL |
|---|---|
| x = ≤100 | x = ≤100 |
| y = 1.5 | y = 1 |
| z = 1 | z = 0.2 |

**Figure 1. Relative composition of uncured DC745U.**

DC745U has been marketed as a material that does not need post-cure conditions.[5] However, post-cure on DC745U has always been used because it is known that it reduces the amount of residual peroxide curing agent, reduces the amount of volatiles, and induces additional crosslinks. However, post-cure studies have not been performed on current DC745U pressure pads. Previous curing studies performed in 1981 at Kansas City Plant (KCP) involved solvent extracts, stress relaxation, and solvent swell tests.[6] These tests were executed on pressure pads made out of Silastic 745U cured with Luperco 101XL. Silastic 745U was the name of the resin

when manufactured in the facility located in Kendaville, IN. The product line was eventually moved to Xiameter® under the name of DC745U. Also, Luperco 101XL (Pennwalt Corp.) is a different peroxide curing agent than what we currently use, Varox DBPH-50 (Vanderbilt Company). Seemingly, the curing/post-curing conditions identified back in 1981 were adapted for the manufacture of current pressure pads. It is known that incomplete curing of the polymer can lead to weak chemical linkages and physical interactions that can negatively affect the polymer's mechanical properties, such as compression set, and thermal properties, e.g., crystallization.[7,8] Also, residual low-molecular-weight volatiles and water create outgassing concerns. This report describes results on studies performed to determine the effect of post-curing on DC745U. Experiments described here include Nuclear Magnetic Resonance (NMR) spectroscopy, Fourier transform infrared (FTIR) spectroscopy, dynamic scanning calorimety (DSC), thermal gravimetric analysis (TGA) coupled with FTIR and mass spectrometry (MS), gas chromatography/mass spectrometry (GC/MS), and mechanical testing.

## 2.0 EXPERIMENTAL INFORMATION

### 2.1 Preparation of DC745U samples

DC745U samples were all prepared from a 6 kg batch at Honeywell's Kansas City Plant. The curing and post-curing conditions are described in Table 1. (The Kansas City Plant production process has been described elsewhere by Denisse Ortiz-Acosta in report W-1-TR-0098U[3] and a *Kansas City Plant Plan Information report*.[7])

**Table 1. Curing and post-curing conditions of DC745U samples used in this study.**

| DC745 sample | Curing conditions | Post-curing conditions |
|---|---|---|
| Raw gum stock | - | - |
| 1003 | 1 h @160ºC | No post-cure |
| 1004 | 1 h @160ºC | 1 h @ 149ºC/ 8 h @ 249ºC |
| 1005 | 1 h @160ºC | 1 h @ 149ºC/ 4 h @ 249ºC |
| 1006 | 1 h @160ºC | 1 h @ 149ºC/ 2 h @ 249ºC |
| 1007 | 1 h @160ºC | 1 h @ 149ºC |

### 2.2 Differential Scanning Calorimetry (DSC)

Differential scanning calorimetry (DSC) was used to determine the glass transition temperature $T_g$, heat of crystallization, and melting point of DC745U samples cured and post-cured under various conditions. The samples were rapidly cooled to -20ºC, and then cooled at 2ºC/min to -150ºC. The samples were equilibrated at -150ºC and then heated at 10ºC/min to 100ºC. The $T_g$ was defined as the mid-point height of the step transition and the heats of crystallization and melting were determined by integrating the endothermic and exothermic peak from -100ºC to -40ºC, respectively.

## 2.3 Thermal Gravimetric Analysis (TGA) Interfaced with FTIR

The thermal decomposition of DC745U and outgas analyses were performed using a TGA Instrument Q5000 interfaced with a Nicolet 380 FTIR. The mass flow and balance flow in the TGA were set to 25 mL/min and 10 mL/min of nitrogen, respectively. The TGA temperature was set to a maximum of 1000°C at a rate of 10°C/min and a final isotherm of 10 min. The samples were placed in a high temperature platinum crucible. The FTIR was equipped with a TGA/FTIR interface gas chamber from ThermoFisher Scientific. The FTIR method used involved 32 scans, a resolution of 4, the step size was 0.646, an aperture of 100, and the detector was DTGS KBR.

## 2.4 Thermal Gravimetric Analysis (TGA) Interfaced with MS

The DC745U samples were analyzed using a Netzsch STA 409 CD thermal analysis instrument. The instrument uses a "skimmer furnace" connected to a Balzers quadrapole mass spectrometer. The skimmer system gives real-time sampling of evolved material from the thermal decomposition of the sample. The quadrapole spectrometer reveals the composition of the evolved material according to the mass-to-charge ratio (m/z) of the molecular fragments.

A Netzsch sample carrier was used along with an alumina sample crucible for the TGA. The sample crucibles were baked out in air at 1200$^{o}$C before being used for TGA analyses. TGA of the DC745U samples was conducted on 20-30 mg samples from 30$^{o}$C to 800$^{o}$C at 10$^{o}$C/min. TGA was carried out under an ultra-high-purity helium atmosphere at a flow rate of 40 to 45 mL/min. A buoyancy correction for the empty sample crucible was used to correct for buoyancy effects in the system. MS data was collected simultaneously with the TGA run. The MS data was set up to "scan bar graph cycles" over a mass-to-charge ratio range of 10 to 300 m/z.

## 2.5 Fourier Transform Infrared (FTIR)

The FTIR spectra were taken in an Avatar System 360 from ThermoFisher Scientist equipped with a Smart DuraSamplIR accessory and a DTGS KBr detector. The system was set up to 50 scans, 8 $cm^{-1}$ resolution, a sample gain of 8, optical velocity of 0.6329, and an aperture of 100.

## 2.6 $^{1}H/^{29}Si$ Cross-Polarization Magic Angle Spinning (CPMAS) Nuclear Magnetic Resonance (NMR)

The experiments were performed on a Bruker 400 MHz solid-state NMR spectrometer. The parameters for the $^{1}H$ were the following: $\pi/2$ was 4.5 μsec, contact time was 5 msec, the samples were spun at 7,000 Hz and the number of acquisitions was 40,000. The frequency for $^{29}Si$ was 79.45 MHz and $^{1}H$ was 399.95 MHz. $^{29}Si$ chemical shifts were referenced to tetrakis (trimethylsilyl) silane.

## 2.7 Solvent Extraction Experiments

The DC745U samples (~0.6 g) were stirred in 2 mL of $CDCl_3$ for 24 hours. The material was dried under vacuum and reweighted. The solvent extract was analyzed by $^{1}H$ and $^{13}C$ NMR spectroscopy and GC/MS.

## 2.8 $^{1}H$ and $^{13}C$ Solution-state Nuclear Magnetic Resonance (NMR)

The experiments were performed on a Bruker 400 MHz NMR spectrometer. The solvent used was $CDCl_3$.

## 2.9 Gas Chromatography/Mass Spectrometry (GC/MS)

Samples were analyzed using a 6890N Gas Chromatograph coupled with a 5973N Mass Spectrometer. The GC was equipped with an Agilent Technologies HP-5MS 30m × 0.25 mm, 2.5 micron film thickness column. The parameters used are the following:

Injection: 1 μL, splitless

Oven: Initial temperature of 45ºC, hold for 5 minutes; ramp at 10ºC/min to 250ºC and hold for 15 minutes. The total run time was 40.5 minutes

Flow: 1.0 mL/min.

## 2.10 Spin-Echo Nuclear Magnetic Resonance Experiments

The experiments were performed on Bruker Minispec ProFiler operating at 15 MHz. The experimental parameters were set as follow: echo time of 0.30 ms with 1200 echoes time per experiment and 128 scans signal averaged per echo time. The echo times were systematically increased until the $T_2$ remained consistent to avoid interfering effects of $T_{1p}$ in Carr-Purcell-Meiboom-Gill (CPMG) experiment. The pulse attenuation, receiver gain, and recycle delay were set to 4 dB, 101 dB, and 1 s, respectively. The spin-echo decay curves were obtained using a Carr-Purcell-Meiboom-Gill pulse sequence. Decay curves were fit to a two-component exponential decay using the Bruker software.

$$E(t) = A_1 \exp(-2t/T_{21}) + A_2 \exp(-2t/T_{22})$$

Further data processing was performed with the Contin application from Bruker Optics, which uses and inverse Laplace transform to yield the distribution of $T_2$ relaxation times.

## 2.11 Variable Temperature $T_2$ Nuclear Magnetic Resonance Experiments

Akin to the relaxation studies at room temperature using the Bruker Minispec Profiler, CPMG $T_2$ variable temperature measurements were done on a Bruker Biospin 300 MHz NMR liquids spectrometer with variable temperature capabilities from -150°C to 150°C. It should be noted that $T_2$ is a measure of the rate at which transverse magnetization is lost in the x-y plane during a NMR experiment as the spins return to equilibrium along the z axis. It is a direct measure of the motional diffusion rates of the polymer and hence the degree of cross-linking. Short $T_2$'s are observed for rigid, crystalline states and long $T_2$'s are found in liquids and plastic phases.

The pulse sequence was the standard CPMG sequence with 8.23 μsec π/2 and 16.46 μsec π pulses for $^{1}H$. A 200 μsec delay was used before and after the π pulses. Probe was tuned at each temperature and different sample to ensure reliable pulse lengths and power levels. A 6.5 s recycle delay was used between acquisitions for full $T_1$ relaxation; $T_1$ was measured to be approximately 1.2 s for $^{1}H$ in this material. Samples were not spun and cooling was achieved under dry nitrogen gas. Samples were held at final temperatures (25°C, -50°C, and -70°C) for 5 min to ensure temperature equilibrium.

### 2.12 Mechanical Tests

Stress-strain curves were obtained at -50ºC. The samples were dwelled for 10 minutes at -50ºC before tests. The samples were cycled three times at a 0.001/s loading/unloading rate. This temperature and strain rate was chosen to determine if a change in the crystalline phase transition could be determined with this technique.

## 3.0 RESULTS AND DISCUSSION

### 3.1 Differential Scanning Calorimetry

The DSC results for samples post-cured under various conditions are summarized in Table 2 and Figure 2.[8] Results indicate that upon heating, the samples show a $T_g$ of -125ºC. $T_g$ is the glass transition temperature of the material, and it is the temperature at which the material loses it elastomeric properties and become glassy or brittle. The $T_m$ (or melting point) observed for all of the samples upon heating was ~ -45ºC. As the polymer is cooled highly organized domains called crystallites are formed as random coil chains become close in proximity. These crystalline domains do not form in the bulk material and only a percentage of the highly organized domains are formed within the polymer. The $T_m$ can be described as the temperature at which the crystalline domains melt, or disappear. The heat of fusion ($\Delta H_f$) observed for all samples was ~ 16.3 J/g. Upon cooling, the heat of crystallization ($\Delta H_{xtal}$) observed was ~ 15.5 J/g.

**Table 2. DSC results for DC745U post-cured under various conditions.**

| S/N | DSC file name | Cooling | | Heating | | |
|---|---|---|---|---|---|---|
| | | $T_c$ (ºC) | $\Delta H_{xtal}$ (J/g) | $T_g$ (ºC) | $T_m$ (ºC) | $\Delta H_f$ (J/g) |
| 1003 | 8BO59A | -64 | 15.9 | -125 | -45 | 16.4 |
| 1004 | 8BO59B | -64 | 14.6 | -125 | -44 | 16.2 |
| 1005 | 8BO59C | -65 | 15.4 | -125 | -45 | 16.6 |
| 1006 | 8BO59D | -64 | 15.8 | -125 | -45 | 16.3 |
| 1007 | 8BO59F | -64 | 15.3 | -126 | -45 | 16.1 |

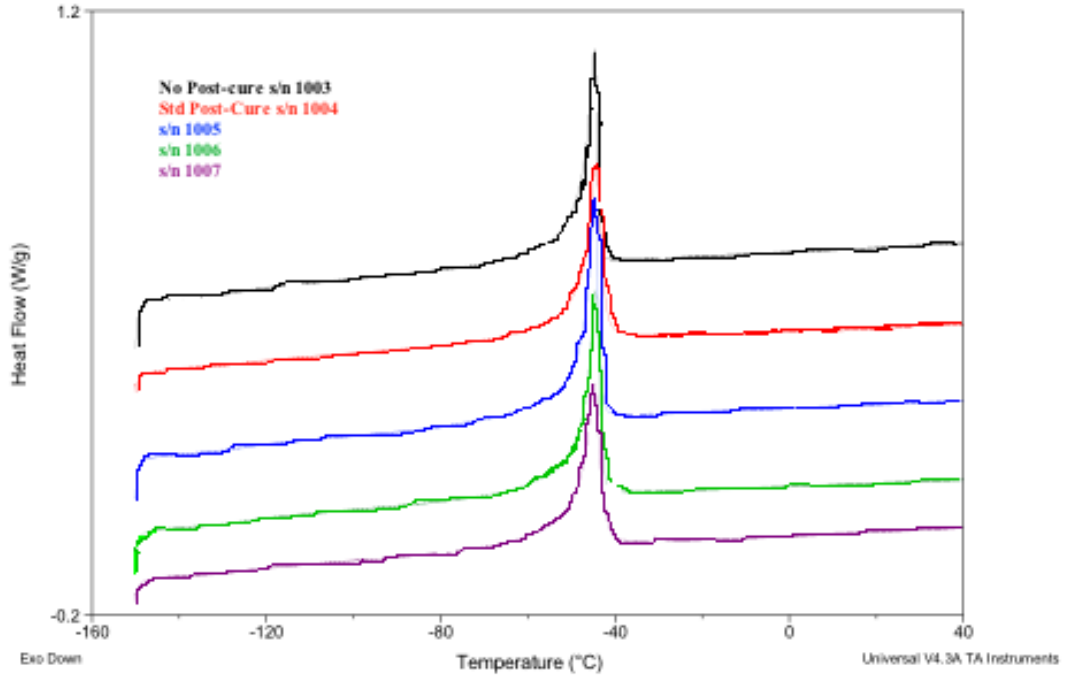


**Figure 2. Subsequent heating of post-cured DC745U samples after controlled cooling.**

The purpose of post-curing is to increase the crosslink density and to reduce volatile materials within the polymers. For instance, the heats of crystallization and fusion are expected to decrease for highly crosslinked polymers. However, the samples displayed no significant differences in the heats of crystallization and fusion, as well as in the $T_g$ and $T_m$. Thus, it was determined that post-cure conditions have no significant effect on crystallinity of DC745U.

## 3.2 TGA/FTIR and TGA/MS

TGA/FTIR and TGA/MS were used to study the decomposition temperature and the outgas products of DC745U cured under different conditions. The results are summarized in Table 3 and show that DC745U decomposes in the TGA/FTIR at an average temperature of 515°C with a weight loss of ~57%. The remaining 42% of material corresponds to the filler. DC745U decomposes in the TGA/MS system at an average temperature of 505ºC with an average weight loss of ~59%. The differences between TGA/FTRI and TGA/MS results are due to different carriers within the systems (He vs. $N_2$). It is observed that uncured DC745U and cured and post-cured elastomer materials have approximately the same decomposition behavior regardless of the curing and post-curing conditions, as shown in Figure 3 and Table 3. The similar decomposition behaviors in the samples indicate that the curing and post-curing conditions do not affect thermal properties of the materials. In addition, little differences in weight loss can be observed before decomposition. This weight loss can be attributed to loss of water and low-molecular-weight compounds. The data suggest that the uncured and cured polymers behave similarly under decomposition conditions. This means that polymer-filler

interactions play an important role in the materials' thermal properties. Yet, the changes in crosslink density compared to the uncured material are enough to change its physical properties going from a putty-like consistency to a firm rubber.

**Table 3. Summary of TGA results on DC745U samples.**

| Material | Onset $T_d$ (°C) (TGA/FTIR) | Weight loss (%) (TGA/FTIR) | Onset $T_d$ (°C) (TGA/MS) | Weight loss (%) (TGA/MS) |
|---|---|---|---|---|
| Raw gum | 517.48 | 56.97 | 503.3 | 59.56 |
| 1003 | 514.06 | 57.27 | 503.8 | 59.06 |
| 1004 | 514.77 | 56.47 | 508.2 | 58.97 |
| 1005 | 516.26 | 56.50 | 503.8 | 58.36 |
| 1006 | 513.80 | 57.06 | 506.3 | 59.18 |
| 1007 | 517.34 | 56.82 | 506.0 | 58.56 |

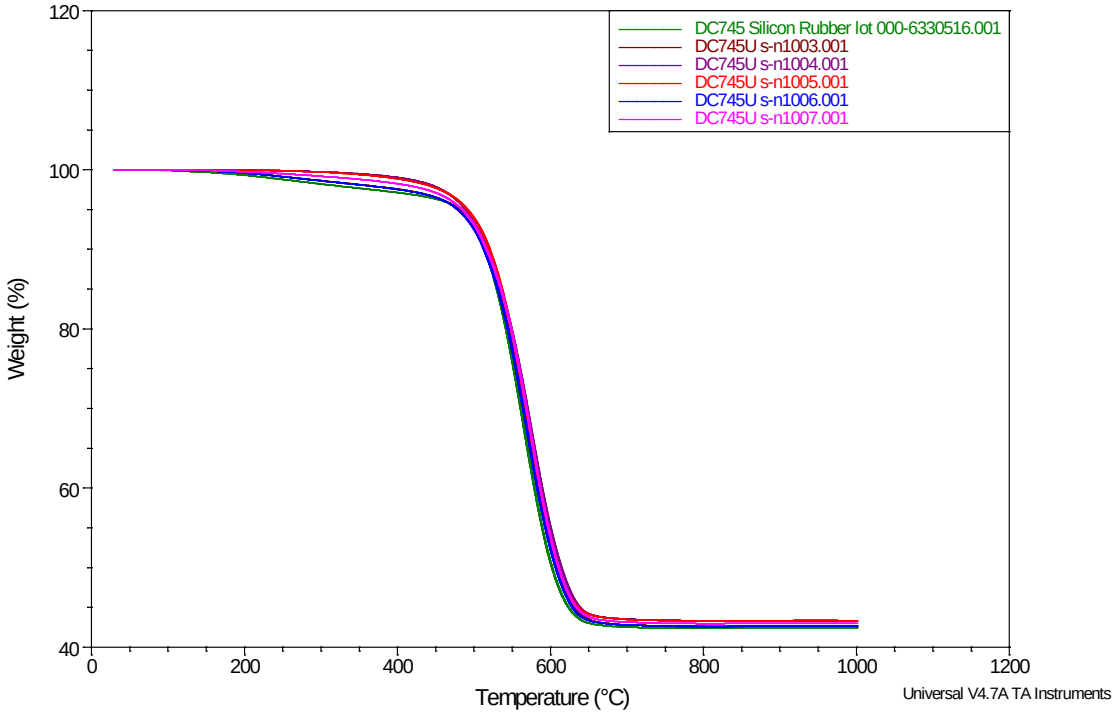


**Figure 3. TGA graph with the decomposition profiles of DC745U materials.**

The outgas analysis for decomposition products of DC745U by gas phase FTIR show that the major loss are cyclic siloxanes. The spectrum obtained for the thermal degradation products of DC745U is shown in Figure 4. The spectrum show peaks at 2910 and 2970 $cm^{-1}$ associated with symmetric and asymmetric C-H stretching bands in $CH_3$ groups, respectively. The peak at 1264 $cm^{-1}$ corresponds to the symmetric deformation of Si-$CH_3$ bonds. The peaks at 1083 and 1024 $cm^{-1}$ are associated with the stretching band of Si-O-Si bonds. The peak at 815 $cm^{-1}$ corresponds to Si-C stretching vibrations. It has been reported that the major loss for silicone elastomers is hexamethylcyclotrisiloxane. However, it is hard to determine the main compound lost by FTIR mostly because of the presence of two peaks in the 1000 $cm^{-1}$ part of the spectrum. The FTIR spectrum of hexamethylcyclotrisiloxane has only one band at 1020 $cm^{-1}$ that corresponds to Si-O-Si stretching vibrations. The presence of two bands in this region, at 1083 and 1024 $cm^{-1}$, indicates that there are other siloxane molecules present in small quantities. Figure 5 shows a representative three-dimensional FTIR spectrum of the lost products as a function of time. The graph shows that the larger quantity of products detected by FTIR occurs at 55 minutes that corresponds to ~513 ºC in the TGA.

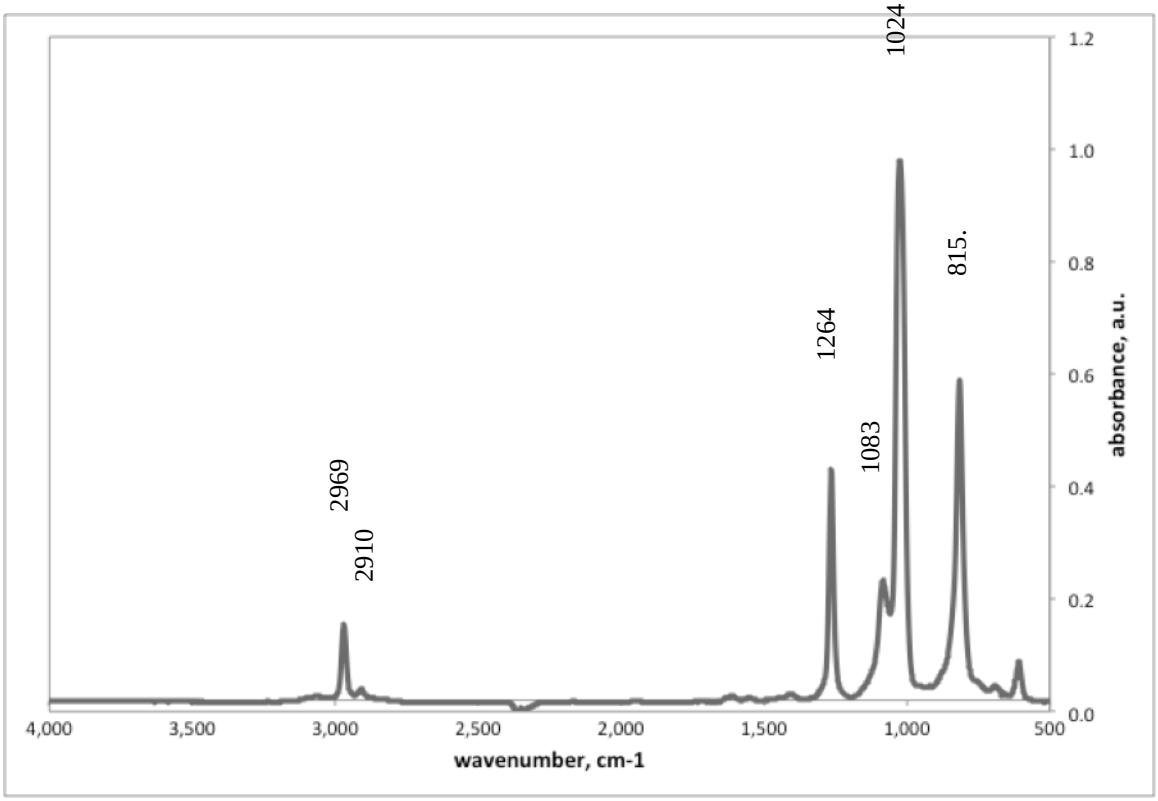


**Figure 4. FTIR spectrum of the degradation product of DC745U.**

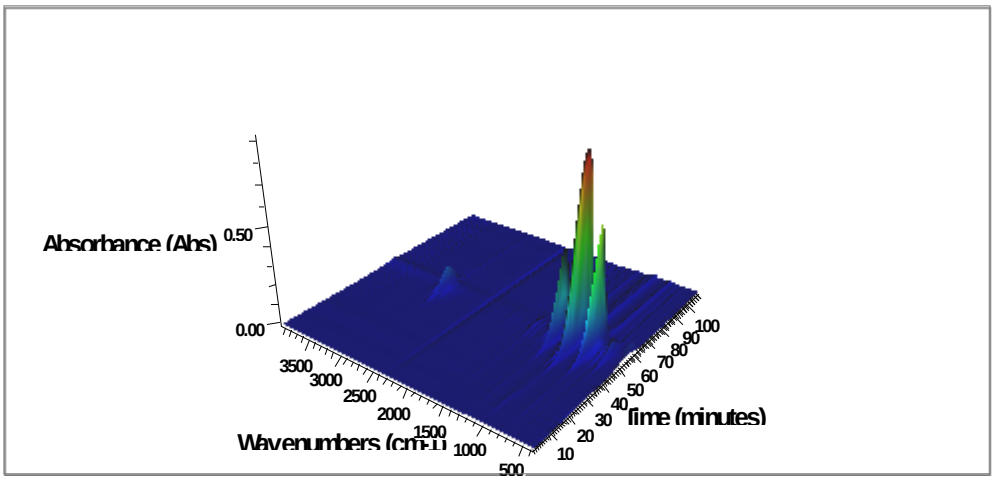


**Figure 5. 3-D FTIR spectrum of degradation product of DC745U.**

The MS data shows a great variety of fragments due to thermal decomposition of DC745U. The most intense mass fragments observed were (m/z) 207, 73, 96, 133, 281, and 75 (in order of decreasing intensity), as shown in Figure 6. The data obtained for all of the samples show that the mass data is consistent. Results show a major loss of m/z 207 that is attributed to the loss of hexamethylcyclotrisiloxane ($D_3$, or three difunctional units of O-Si-O) species. The $D_3$ species can arise from the decomposition of the silicone elastomer and can also be a fragmentation product of octamethylcyclotetrasiloxane ($D_4$) with an m/z of 281. The second most abundant decomposition mass fragments, m/z 73 that arises from trimethylsilyl chain ends on the silicone elastomer. The other products observed arise mostly from $D_3$ and $D_4$ fragmentation.

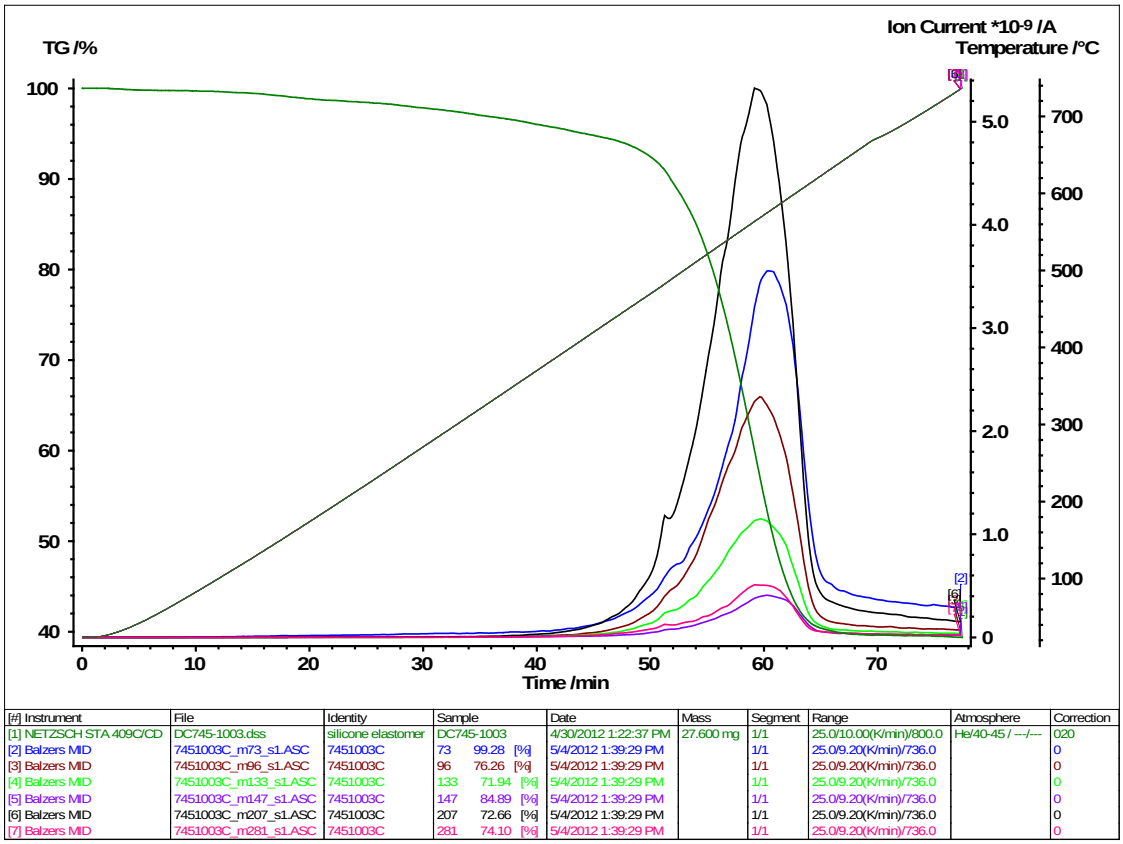


| [#] Instrument | File | Identity | Sample | Date | Mass | Segment | Range | Atmosphere | Correction |
|---|---|---|---|---|---|---|---|---|---|
| [1] NETZSCH STA 409C/CD | DC745-1003.dss | silicone elastomer | DC745-1003 | 4/30/2012 1:22:37 PM | 27.600 mg | 1/1 | 25.0/10.00(K/min)/800.0 | He/40-45 / ---/--- | 020 |
| [2] Balzers MID | 7451003C_m73_s1.ASC | 7451003C | 73 99.28 [%] | 5/4/2012 1:39:29 PM | | 1/1 | 25.0/9.20(K/min)/736.0 | | 0 |
| [3] Balzers MID | 7451003C_m96_s1.ASC | 7451003C | 96 76.26 [%] | 5/4/2012 1:39:29 PM | | 1/1 | 25.0/9.20(K/min)/736.0 | | 0 |
| [4] Balzers MID | 7451003C_m133_s1.ASC | 7451003C | 133 71.94 [%] | 5/4/2012 1:39:29 PM | | 1/1 | 25.0/9.20(K/min)/736.0 | | 0 |
| [5] Balzers MID | 7451003C_m147_s1.ASC | 7451003C | 147 84.89 [%] | 5/4/2012 1:39:29 PM | | 1/1 | 25.0/9.20(K/min)/736.0 | | 0 |
| [6] Balzers MID | 7451003C_m207_s1.ASC | 7451003C | 207 72.66 [%] | 5/4/2012 1:39:29 PM | | 1/1 | 25.0/9.20(K/min)/736.0 | | 0 |
| [7] Balzers MID | 7451003C_m281_s1.ASC | 7451003C | 281 74.10 [%] | 5/4/2012 1:39:29 PM | | 1/1 | 25.0/9.20(K/min)/736.0 | | 0 |

**Figure 6. TGA/MS for DC745U s/n 1003 (similar for all samples).**

The thermal degradation mechanism of silicone elastomers has been described previously.[2] It has been proposed that the mechanism involves chain scissioning and backbitting of the polymer chains, as shown in Scheme 1, releasing low-molecular-weight cyclic siloxanes as major products.

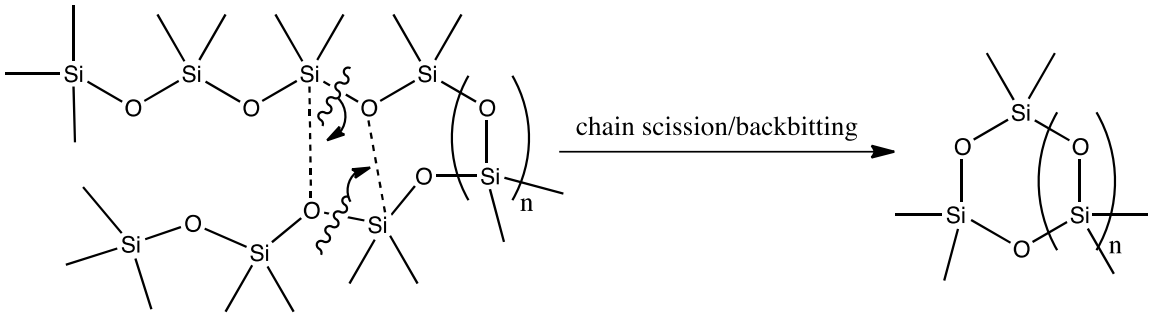


**Scheme 1. Degradation mechanism of silicone elastomers.**

## 3.3 Fourier Transform Infrared (FTIR)

The DC745U samples were analyzed in the top and bottom of the materials, Figure 7. The spectra are representative for silicone elastomers in general. The peak observed at

866 $cm^{-1}$ is assigned to asymmetric stretching of Si-OH bonds. The peak at 1008 $cm^{-1}$ corresponds to stretching vibrations of Si-O-Si, and the peak at 1258 $cm^{-1}$ and 1408 $cm^{-1}$ correspond to symmetric and asymmetric deformations of $CH_3$ groups, respectively. The peak at 1448 $cm^{-1}$ is attributed to bending of C=C-H. Lastly, the peaks at 2905 $cm^{-1}$ and 2963 $cm^{-1}$ are assigned to symmetric and asymmetric stretching vibrations of methyl groups.

Changes to the IR spectra were observed mostly on the bottom part of the materials, as shown in Figure 7. Note on Figure 7a that the spectra from the top of DC745U materials show no apparent differences. The spectra of the bottom of the materials show differences that are more obvious at 1448 $cm^{-1}$. This region is observed to be larger for the no post-cured elastomer and its area decreases for the post-cured samples. These differences suggest reduced vinyl content for the materials that were post-cured for longer time and at higher temperature during production. Differences between top and bottom of the samples could be attributed to the manufacturing process (e.g., heat distribution, molds, fiber mat, etc.).

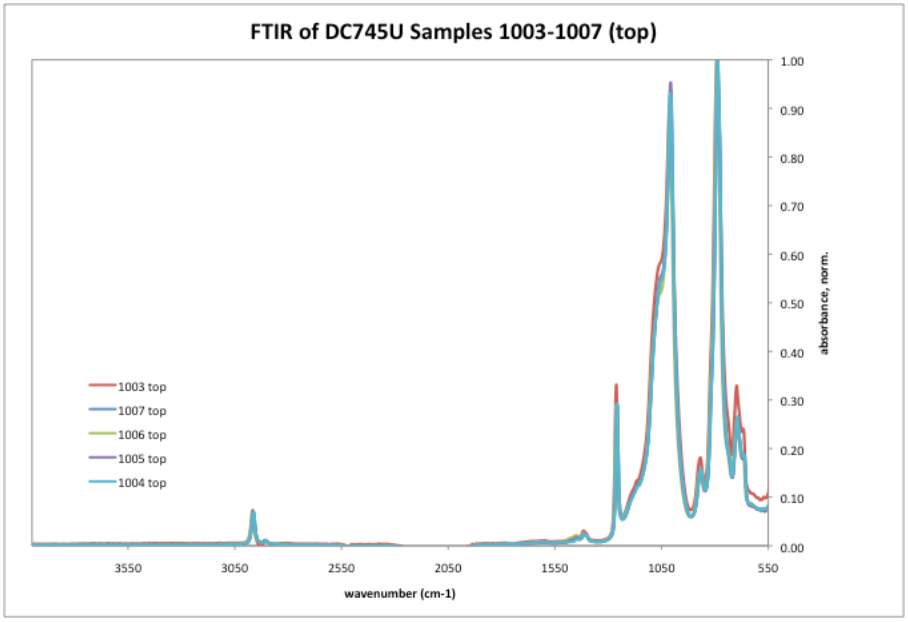

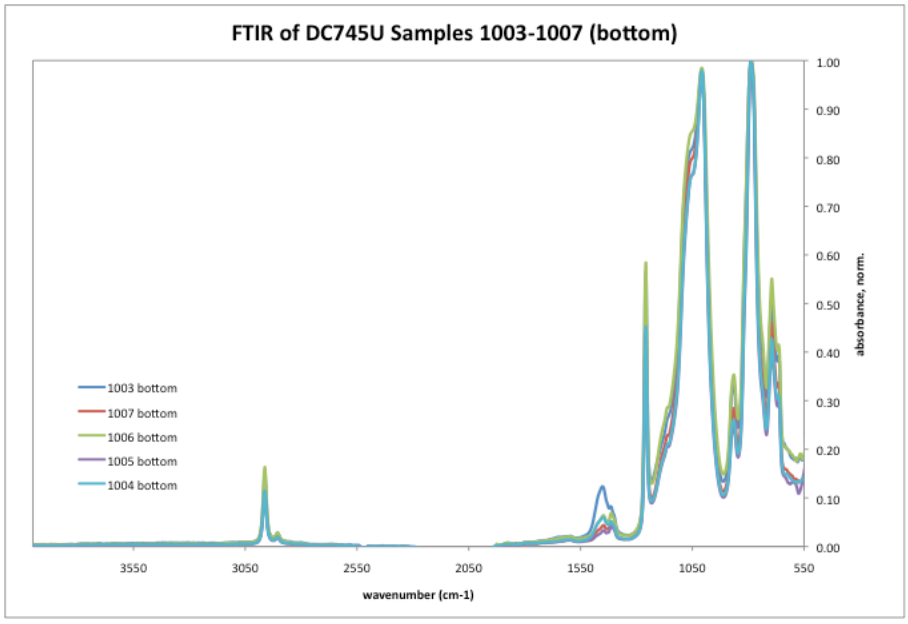


**Figure 7. FTIR spectra for DC745U samples post-cured under various conditions on top (a) and bottom (b) of the samples.**

The difference in spectra between the top and bottom of the samples could be explained by the fact that the bottom parts of the samples are in closer proximity to the fiber mat. Perhaps, the fiber mat has some effects on the curing process of DC745U.

## 3.4 $^{29}$Si Cross-Polarization Magic Angle Spinning-NMR

$^{1}$H/$^{29}$Si cross-polarization magic angle spinning (CPMAS) NMR spectroscopy was used to achieve an increase in signal-to-noise and a decrease in any signals that correspond to the mobile phase of the polymer network. It allows the analysis of the polymer-filler interface by enhancing the signal of the inorganic and substituted components of the polymer. This technique, while qualitative, also provides information about the mobility of the polymer. In general, the more mobile the polymer is, the less cross-polarization occurs within the nuclei and the smaller the peaks are. The $^{29}$Si CPMAS NMR spectra for the DC745U samples are shown in Figure 8. The chemical shifts for the uncured and cured materials are nearly identical and show peaks at -25 ppm, -35 ppm, -100 ppm, and -110 ppm that correspond to methyl groups, phenyl groups, and silicates (-100 and -110 ppm), respectively. Similar results were described previously by R. Iuliucci et al.,[9] who suggested that the similarities in spectra between the cured and uncured materials are due to a nonchemical surface-binding mechanism that involves hydrogen bonding, van der Waal forces, entanglements, and polymer-filler interactions. The methyl group signal at -25 ppm is smaller for the uncured sample due to the fact that the uncured material has more mobility of the polymer resulting in less polarization during cross-polarization (cp) experiments.

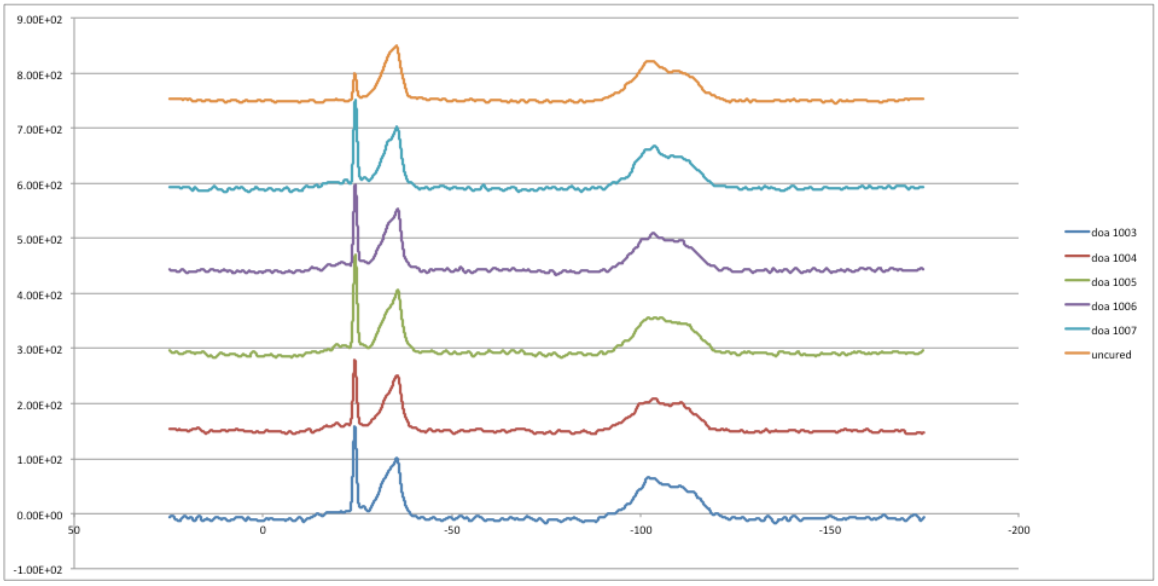


**Figure 8. $^{29}$Si CPMAS NMR spectra for DC745U samples cured and post-cured under various conditions.**

## 3.5 Solvent Extraction Experiments

DC745U was extracted using $CDCl_3$ to be able to determine the amount of extractable material present in the different samples, while at the same time allowing for NMR analysis and GC/MS. Amounts of ~ 0.65 g of DC745U were stirred over 2 mL of $CDCl_3$ for 24 hours. Then, the samples were dried under vacuum, reweighed, and analyzed. Results are shown in Table 4. Results show that post-curing conditions do have an effect on the amount of extractable materials on the final product. There is a decrease in extractable material for samples cured for longer periods of times and at higher temperatures. Sample 1004, which was cured under standard production conditions, has the least amount of unbounded species. Unbound, low-molecular-weight compounds could potentially cause problems when the material is integrated into the system causing outgassing and possibly corrosion.

**Table 4. Unbound, extractable material on DC745U samples cured under various conditions.**

| Sample | Initial weight (g) | Final weight (g) | % Extractable material |
|---|---|---|---|
| 1003 | 0.06341 | 0.05777 | 8.9 |
| 1004 | 0.6809 | 0.6383 | 6.3 |
| 1005 | 0.06670 | 0.06232 | 6.6 |
| 1006 | 0.06359 | 0.05851 | 8.0 |
| 1007 | 0.06413 | 0.05811 | 9.4 |

## 3.6 $^{1}$H and $^{13}$C Nuclear Magnetic Resonance of Extracted Material

Extracted material obtained from DC745U samples cured and post-cured under different conditions was analyzed by $^{1}$H-NMR and $^{13}$C-NMR. The $^{1}$H-NMR spectra are shown in Figure 9. The spectra show peaks at 0 ppm that corresponds to dimethylsiloxane group. The peaks between 0 and 2 ppm correspond to silanol, siloxane oligomers, and water. The peaks between 7 and 8 ppm are attributed to phenyl protons. The uncured sample also shows peaks between 5 and 6 ppm that correspond to vinyl groups. Results show that the samples do have low-molecular-weight materials that can be extracted. The amount of extractable material decreases with increasing post-cure to standard conditions (s/n 1004). This suggests that post-cure is necessary on DC745U and reduces the presence of low-molecular-weight compound that could potentially outgas while in the system.

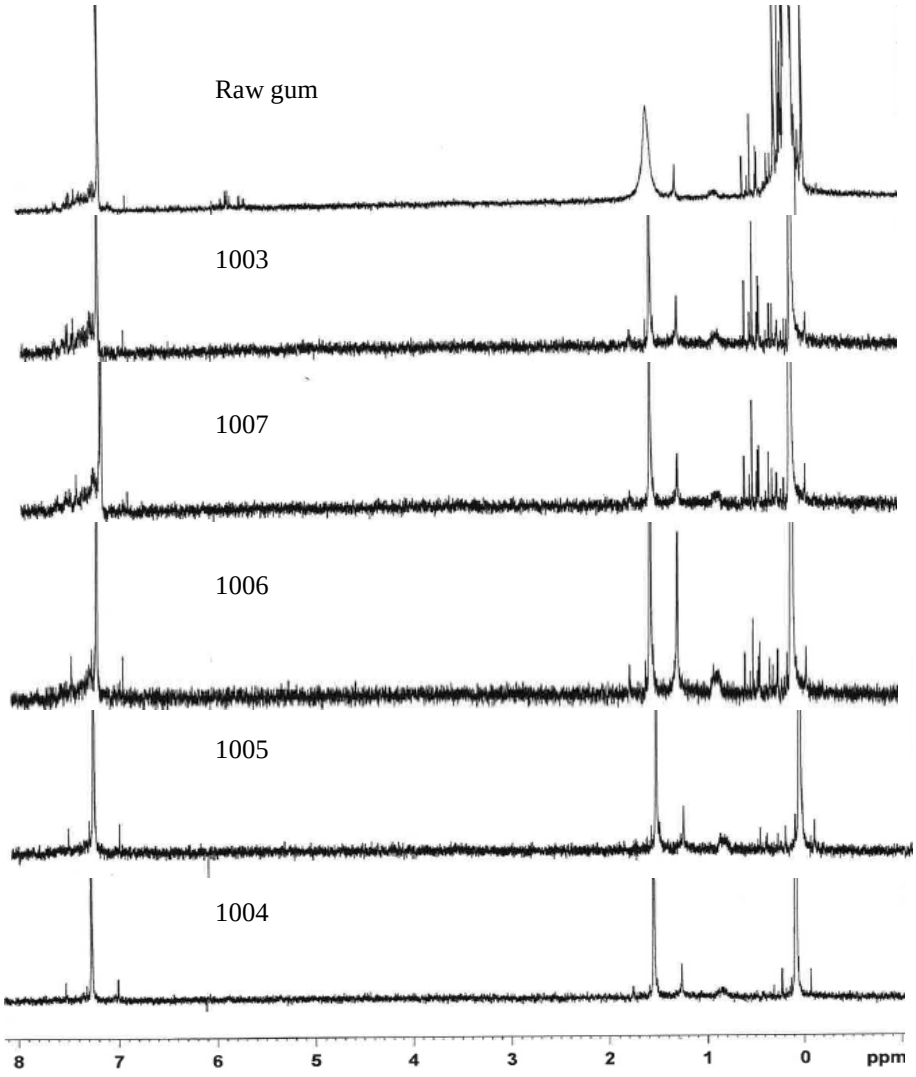


**Figure 9. $^{1}$H-NMR spectra of extracted material from DC745U samples.**

$^{13}$C-NMR spectra do not show differences between the samples. A peak at ~ 1 ppm is observed and corresponds to the methyl groups in PDMS. The peaks at 77 ppm correspond to the solvent, $CDCl_3$. A representative $^{13}$C-NMR spectrum is shown in Figure 10.

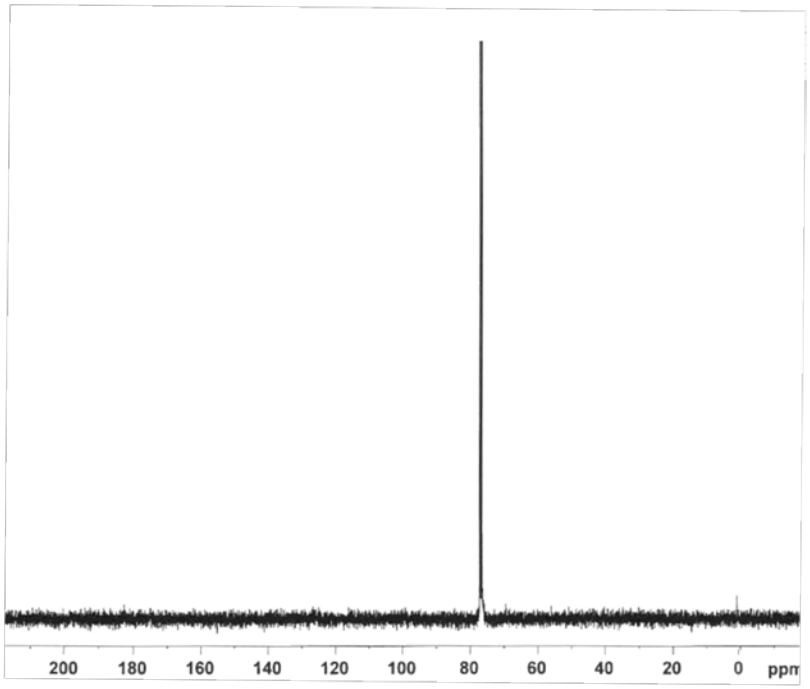


**Figure 10. Representative $^{13}$C-NMR spectrum for DC745U samples 1003-1007.**

## 3.7 Gas Chromatography/Mass Spectrometry

GC/MS was also used to determine the identity of the material extracted from DC745U samples. Results confirmed the presence of cyclic siloxane with lower quantities for materials cured for longer period of times (s/n 1004). These observations are parallel with the ones obtained using $^{1}$H-NMR spectroscopy and solvent extraction analysis. The most common compounds present in the extracts are decamethyl cyclopentasiloxane, dodecamethyl cyclohexasiloxane, tetradecamethyl cycloheptasiloxane, hexadecamethylcyclooctasiloxane, octadecamethyl cyclononasiloxane, eicosamethyl cyclodecasiloxane, and 2,4,6-trimethyl-2,4,6-triphenyl cyclotrisiloxane. These compounds may have come from starting materials used by Dow Corning to synthesize the base polymer.

## 3.8 Spin-echo Nuclear Magnetic Resonance Studies

NMR spectroscopy is a common technique used to study the chemical structure and composition of compounds. Recently, spin-echo NMR spectroscopy has found application in the study of polymer's molecular properties, such as crosslink density, mobility, and diffusion. Thermal, mechanical, and physical properties of polymers are determined by molecular dynamics within the polymer network. Spin-echo experiments give information about spin-lattice ($T_1$) and spin-spin ($T_2$) relaxation times, which can provide insights into curing behavior, heterogeneities, damages and defects within the polymer by studying the molecular properties described above. Spin-lattice relaxation time, $T_1$, is governed by fast main chain rotations at high fields, while at low fields it is sensitive to both fast and slow dynamics. The spin-spin relaxation time, $T_2$, is sensitive to

slower translational motions that are constantly changing due to the dynamic nature of polymers. In the study of DC745U samples we used a Bruker Minispec ProFiler, a 400 MHz solid state NMR, and a Stelar SmartTracer field cycling NMR relaxometer to obtain information on mobility and crosslink density on the samples cured under different conditions by determining their spin-spin and spin-lattice relaxation times, $T_2$ and $T_1$, respectively.

The Bruker Minispec ProFiler is a hand-held NMR instrument that does not require sample preparation and which uses a very low frequency of 15 MHz to analyze the materials. The decay curves obtained for the different DC745U samples are shown in Figure 11. The data shows that there are two relaxation time components, $T_{21}$ and $T_{22}$. The $T_{21}$ components is designated as the short component and is attributed to protons that exist within the network structure. The network structure consists of crosslinks, entanglements, filler and polymer/filler interactions. Because of the restricted mobility of the polymer in the network structure and near surroundings, its relaxation time decays rapidly. The $T_{22}$ relaxation time describes the long component and represents the mobile, non-network polymer chains. Due to the freedom in motion in non-network polymer chains, the relaxation time of protons existing in the non-network environment relaxes slowly.

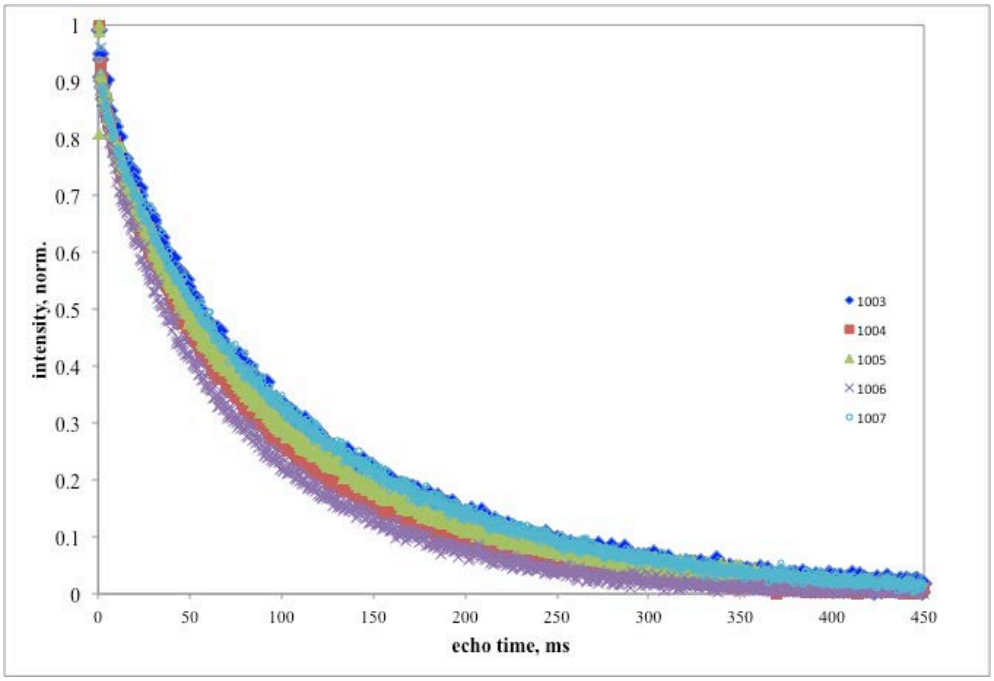


**Figure 11. $T_2$ relaxation time data for DC745U samples 1003-1007 using a 15 MHz Minispec ProFiler.**

The $T_{22}$ results using the Minispec ProFiler show that the sample cured under standard conditions, 1004, has the shortest $T_2$ value, as shown in Table 5. Short $T_2$ relaxation time values indicate a decrease in mobility of the polymer chains. Samples 1003 and 1007 show similar chemical behaviors with longer $T_2$ values. The longer $T_2$ values indicate more mobility of the polymer chains. These results are expected since one of the

functions of post-curing is to induce higher crosslink density. Ordinarily, for polymers that contain both network and non-network systems the two relaxation time components are related to each other. This means that if more of the long component, $T_{22}$, is present, then the short component $T_{21}$ value should increase because the mobility of the network is enhanced by the more mobile polymer chains. However, the $T_{21}$ relaxation times are not affected by post-cure conditions and no correlation exists between $T_{21}$ and $T_{22}$ decays. This is because in filled polymers like DC745U the short relaxation component of governed by the filler and filler-polymer interactions and this interactions do not necessarily change with small changes to the crosslink density of the material. Therefore, we can assume that the most important changes occur in the mobile phase of the resin.

**Table 5. Summary of the data obtained for DC745U samples using the Minispec ProFiler.**

| Samples | $A_{21}$ (%) | $T_{21}$ (ms) | $A_{22}$ (%) | $T_{22}$ (ms) |
|---|---|---|---|---|
| 1003 | 5.06 | 17.66 | 25.78 | 113.54 |
| 1004 | 6.06 | 16.16 | 27.02 | 96.39 |
| 1005 | 4.81 | 10.82 | 27.51 | 97.12 |
| 1006 | 5.12 | 14.37 | 28.13 | 103.05 |
| 1007 | 5.12 | 17.72 | 27.95 | 116.71 |

High-field solid-state NMR was also used to obtain complementary information on the materials' molecular behavior. At high-magnetic field information on the dynamics of short-range chains and intramolecular interactions can be obtained. Data obtained at high-field NMR on DC745U, Figure 12 and Table 6, shows that the $T_2$ relaxation times are shorter for samples 1004 and 1005, which behave similarly. Samples 1003 and 1007 also behave similarly with longer $T_2$ values. The fact that samples 1003 and 1007 behave comparable indicates that one hour of post-curing conditions do not induce substantial changes to the chemistry of the polymer. The same reasoning could be applied to samples 1004 and 1005. However, significant changes in the chemistry happen between samples 1003 and 1004 indicating that post-curing at higher temperatures and longer time to standard conditions produces a more stable polymer material. Information obtained using high-field NMR is in agreement with the data obtained using the Minispec ProFiler at 15 MHz.

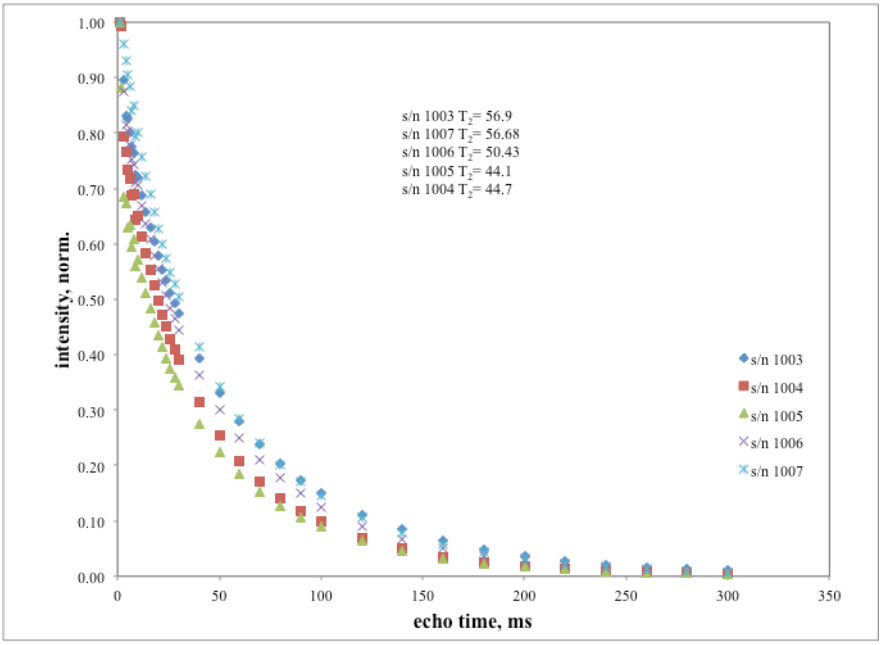


**Figure 12. $T_2$ relaxation decay for DC745U samples 1003-1007 using a 400 MHz Solid-State NMR Spectrometer.**

**Table 6. Spin-spin ($T_2$) and Spin-lattice ($T_1$) relaxation time values for DC745U samples 1003-1007.**

| Sample | Minispec Profiler $T_2$ (ms) | High Field $T_2$ (ms) | Stelar SmartTracer $T_1$ (at 10 kHz, ms) |
|---|---|---|---|
| 1003 | 113.54 | 56.9 | 64 |
| 1004 | 96.39 | 44.7 | 60 |
| 1005 | 97.12 | 44.1 | 62 |
| 1006 | 103.05 | 50.68 | 64 |
| 1007 | 116.71 | 56.9 | 65 |

Spin lattice relaxation times, $T_1$,were obtained using a Stelar SmartTracer field cycling NMR relaxometer. The materials were analyzed using a Nuclear Magnetic Relaxation Dispersion (NMRD) technique. This technique determines $T_1$ values at a wide magnetic field range of 0.002 MHz to 10 MHz (proton frequency). The low magnetic fields used in this study provide information on the polymer's chain modes, intermolecular interactions, and diffusion that are dictated by slow and fast motional dynamics. Results show that $T_1$ at low fields display modest but significant divergence between the different DC745U samples, as shown in Figure 13. The decreasing order of $T_1$ relaxation times is 1007, 1006, 1003, 1005, and 1004, and Table 6 shows the $T_1$ values at 10 kHz. The data converges at 0.1 MHz after which $T_1$ values do not change significantly between samples. The fact that the Stelar data converge past 0.1 MHz indicates that crosslink density is not affecting anything on timescales shorter than 10 microseconds.

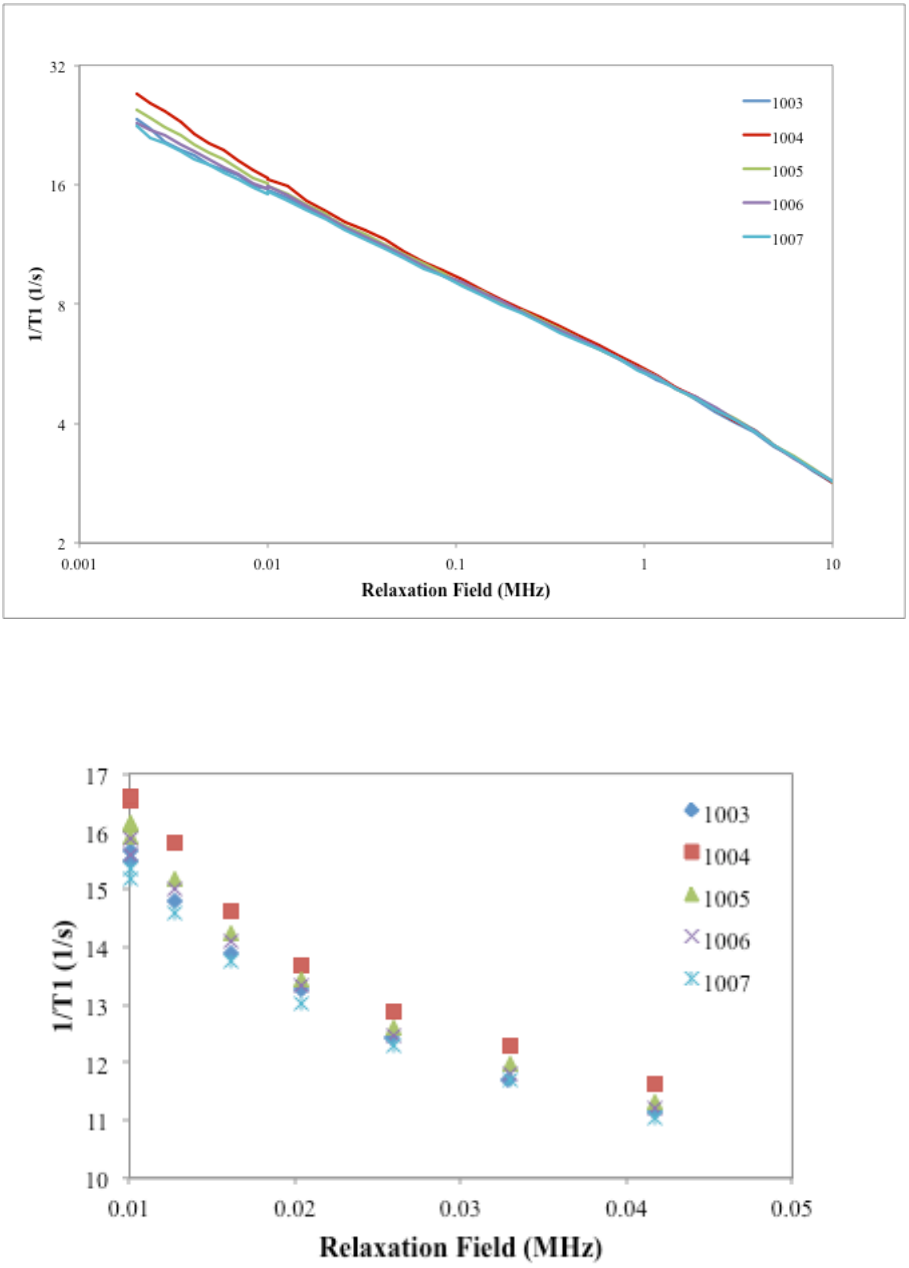


**Figure 13. Spin-lattice $T_1$ relaxation time data for DC745U samples 1003-1007. (Top represents data obtained over a magnetic field of 0.002MHz and 10 MHz. Bottom represents the blown up data at a field between 0.01 and 0.042 MHz.)**

Data obtained using the Stelar system mostly agree with the results obtained using the high-resolution NMR and the Minispec ProFiler. The fully cured sample (1004) shows the shortest relaxation time of 60 ms, followed by sample 1005 with a $T_1$ of 62 ms. The shorter relaxation time means that there is less mobility of the polymer due to a higher crosslink density of the material. Samples 1003, 1006, and 1007 have similar $T_1$ relaxation times. This is because at such low frequencies small changes in crosslink

density does not impact the motion of the polymer, considering that there are many Kuhn segments between crosslinks.

## 3.9 Variable Temperature $T_2$ NMR

$T_2$ measurements for $^1H$ were performed on three DC745U samples to observe phase transition due to the formation of crystalline domains and if there is permanent damage induced with excursions to low temperatures. The three samples were:

- s/n 1003: No post-cure
- s/n 1007: Post-cured with conditions of 1 h @ 300°F
- s/n 1004: Post-cured with conditions of 1 h @ 300°F and 8 h @ 480°F

The three were selected to represent no post-cure (1003), mildest post-cure (1007), and the fully post-cured (1004).

The initial data at 25ºC is summarized in Figure 14. The plot is the intensity of the echo height in the CPMG experiment as it decays with time for the three samples. Samples 1003 and 1007 show similar behavior at room temperature with sample 1004 displaying a faster exponential decay indicative of a higher degree of crosslinking for the longer cure time at higher temperature. Similarities between samples 1003 and 1007 at room temperature have been observed using the different NMR techniques; and sample 1004 has always shown faster echo decays.

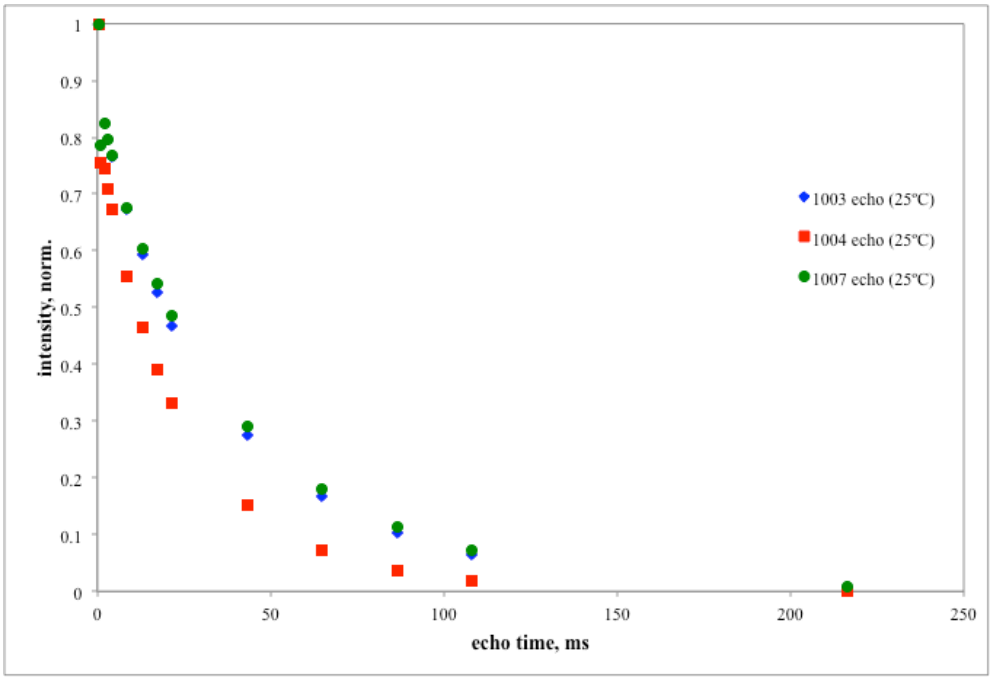


**Figure 14. Variable Temperature NMR experiments at 25ºC.**

The plot in Figure 15 is the $T_2$ experiment measured at -50°C. The decays for the samples are much faster, but a surprising difference can be noted. At room temperature, samples 1003 and 1007 had similar decay rates. *At -50°C, however, 1004 and 1007 display nearly*

*identical behavior*. At this temperature, one can then expect the polymer properties for the two post-cured materials to be similar with substantial differences for the non post-cured 1003 sample. The shorter decay times observed for the three samples at -50ºC indicates stiffening of the polymer, possibly due to the formation of crystalline domains. The fact that the post-cured samples decay much faster than the non post-cured sample indicate that additional crosslinks are being added during the post-curing conditions that affects the polymer's network structure.

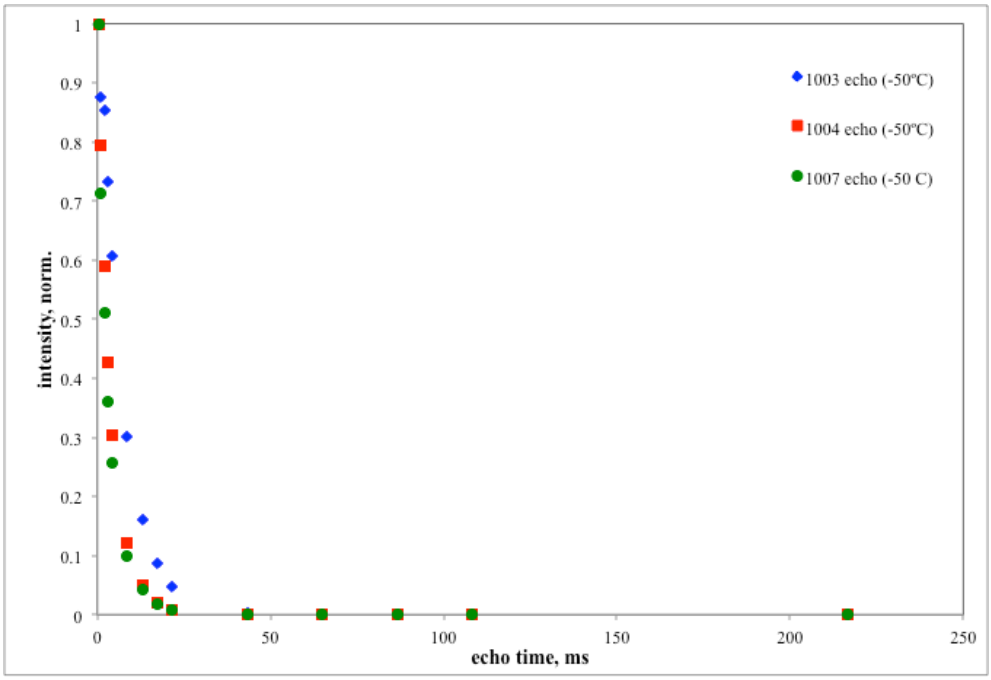


**Figure 15. Variable Temperature NMR experiments at -50ºC.**

The temperature was then decreased to -70°C, Figure 16. At this temperature the $T_2$ is very short for all of the materials, which is expected because the temperature is below the known crystallization temperature. Crystallization of DC745U has been shown to occur between -60ºC and -50ºC under compression.[10] One can assume that all samples behave similarly at temperatures below $T_c$ when complete crystallization is achieved.

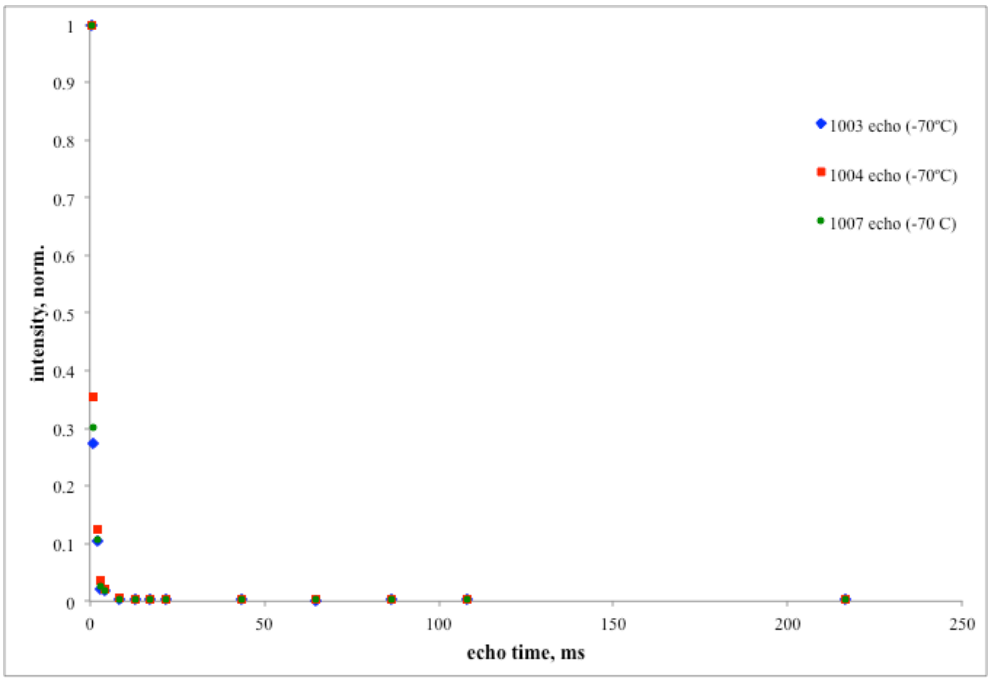


**Figure 16. Variable Temperature NMR experiments at -70ºC.**

The decay curves for the echo intensities were analyzed with a simple exponential decay

$$y = y_o + Ae^{-x/t}$$
$$(echo\ height) = (echo\ height)_o + Ae^{-time/T_2}$$

and $T_2$ values were determined. Decay functions with multiple terms such as a biexponential decay function did not qualitatively change the results or give any insight into the relaxation processes. Table 7 summarizes the $T_2$ values obtained for the different samples. In general, the fully post-cured 1004 sample shows shorter $T_2$ values due to a higher crosslink density. Samples 1003 and 1007 are similar at room temperature, samples 1007 and 1004 are similar at -50°C, and all samples $T_2$ values are similar at -70°C when complete crystallization is reached. It seems like the 1003 sample requires longer time to reach equilibrium at -50ºC due to a higher mobility of the polymer chains, and thus higher $T_2$ values. It would be interesting to see if sample 1003 would reach similar $T_2$ values to 1004 and 1007 at -50ºC over a longer period of time. $T_2$ values return to near original values upon heating to room temperature indicating that the materials recover their chemical properties.

**Table 7. $T_2$ values as a function of temperature for the DC745U samples.**

| | $T_2$ (ms) at temperature | | | | | |
|---|---|---|---|---|---|---|
| **Samples** | **25°C** | **-50°C** | **-70°C** | **25°C (return, 5min)** | **25°C (return, 18min)** | **25°C (return, 30min)** |
| 1003 | 33.46 | 7.37 | 0.52 | 31.79 | 33.05 | 30.52 |
| 1004 | 20.50 | 3.36 | 0.67 | 18.84 | 19.21 | 19.80 |
| 1007 | 35.79 | 2.79 | 0.57 | 34.54 | 34.92 | 36.43 |

### 3.10 Mechanical Tests

Stress-strain curves were obtained on all samples at -50ºC. Experiments were conducted by holding the material at -50ºC for 10 minutes. The samples were then cycled three times at a loading/unloading strain rate of 0.001/s up to transition. Figure 17 shows the first cycle of each sample with different curing conditions. It can be observed that the initial loading modulus for all samples is consistent, up to ~ 25% strain. However, variations in the final strain are observed due differences in time at which the samples came in first contact with the loading platen. Variations in time at temperature could arise from already cold platens, less time necessary to reach the test temperature, fluctuations in temperature before the dwell time that changes the exposure time. It could aso be that the phase transition kinetics for the different samples is different and higher for the 1004 sample.

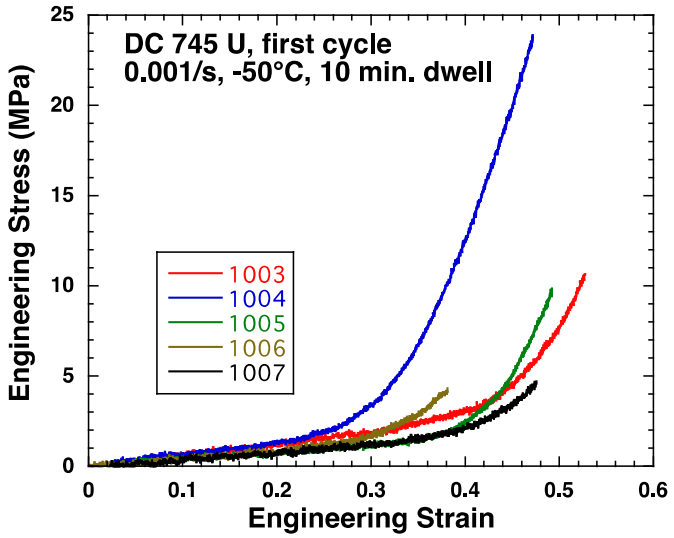


**Figure 17. Stress-strain chart of the first cycle of DC745U samples 1003–1007 ran at -50ºC.**

Figure 18 shows the unloading of the first cycle and all subsequent cycles. It seems that for sample 1004 the second and third cycles reach the same load. Because the first cycle and subsequent cycles did not change significantly, it is assumed that the test was initiated at a time when the crystalline transition had progressed further and differences are difficult to determine. The other samples (1003, 1005, 1006 and 1007) show progressive strengthening from the first cycle to the third cycle. There is also an increase in stiffness (slope) from the second to the third cycles. The unloading modulus seems to be the same for all tested samples and the unloading of the final cycle seems to the the most similar to each other. It can also be observed that the different curing conditions did not affect the phase transition of the material, a behavior also observed by DSC. However, the fully cured/post-cured sample 1004 shows a higher modulus/stiffness at transition. This result agrees with results from all previous experiments, which suggest that the 1004 sample has a higher crosslink density and thus a more rigid polymer network. All other samples show a decrease in modulus at phase transition, possibly due to incomplete curing of the polymer as observed by NMR spectroscopy. All other variations may be tied to time at temperature and other experiments should be considered. Experiments at temperatures below the transition temperature with longer dwell time to ensure full transition prior testing are suggested. In addition, experiments at warmer temperatures are recommended to verify behavior above phase transition.

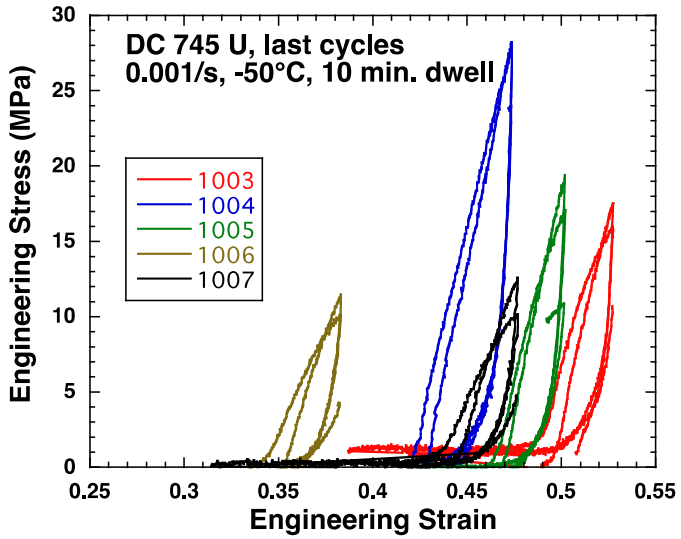


**Figure 18. Stress-strain chart for the inloading of the first cycle and subsequent cycles for DC745U samples 1003–1007.**

## 4.0 CONCLUSIONS

Different techniques were used to perform post-cure studies on the molecular and thermal properties of DC745U. Results are summarized below:

1. DSC show no significant differences on crystallinity for the samples cured and post-cured under various conditions.

2. TGA did not reveal any significant differences on the decomposition behavior between samples.
3. TGA/FTIR and TGA/MS show that the main degradation product of DC745U are cyclic siloxanes.
4. TGA shows small differences in weight loss between samples before decomposition. This weight loss is attributed to loss of low-molecular-weight compounds and water.
5. Solvent extraction experiments show a decrease in extractable material for the samples post-cured for longer times.
6. Solvent phase NMR spectroscopy and GC/MS revealed that the extracted material are mostly low-molecular-weight cyclic siloxanes and oligomers.
7. Spin-echo NMR experiments show an increase in crosslink density for the materials cured for longer time, with higher crosslink density for sample 1004 cured and post-cured under standard conditions.
8. Variable temperature NMR experiments show that DC745U undergoes stiffening at temperatures $\leq 50$ºC. The material recovers to its original state at room temperature.
9. Stress-strain curves show that the different curing/post-curing conditions did not significantly affect the phase transition of the material. The fully cured/post-cured 1004 sample shows the higher stiffness due to a more rigid polymer network.

NMR and FTIR techniques used in this study were able to see the small changes in crosslink density and changes to the polymer network. NMR and FTIR showed the differences in the chemistry of the different samples. However, it seems like these differences are small and do not significantly impact the mechanical and thermal properties studies herein. It was observed that increased post-curing time slightly increases crosslink density and reduces the amount of volatiles. It is also known that post-cure of siloxane polymers reduces the amount of residual peroxide species. Higher crosslink density, low volatile content and absence of peroxide initiator all contribute to low compression set and outgassing. These post-cured studies and its finding demonstrate that the standard curing and post-curing conditions used in Honeywell's Kansas City Plant improve the materials overall properties and should be followed in future production of DC745U components.[5,6]

## 5.0 FUTURE STUDIES

The following future studies are recommended to improve our understanding of DC745U for systems engineering, surveillance, aging assessments, and lifetime assessments:

1. Stress-strain experiments at room temperature and temperature below phase transition for the samples with different curing/post-curing conditions.
2. Thermal aging studies (>6 months) (to begin in FY14)
3. Radiolytic aging studies at lower dose rates and total dose (In Progress).
4. Gather data needed to improve current models- for systems, components and materials.

## 6.0 REFERENCES

(1) Labouriau, A. *DC745*, Los Alamos National Laboratory, 2011.

(2) Maxwell, R. S.; Chinn, S. C.; Herberg, J.; Harvey, C.; Alviso, C.; Vance, A.; Cohenour, R.; Wilson, M.; Solyom, D. *Baseline and Lifetime Assessments for DC745U Elastomeric Components*, Lawrence Livermore National Laboratory, 2005.

(3) Ortiz-Acosta, D.; Densmore, C. G. *Historical Material Analysis of DC745U Pressure Pads*, Los Alamos National Laboratory, 2012.

(4) Ortiz-Acosta, D.; Densmore, C. G. *Solid Silicone Elastomer Material (DC745U)-Historical Overview and New Experimental Results*, Los Alamos National Laboratory, 2012.

(5) Thomas, D. K.; Kay, E. *Compression Set Resistance in Silicone Rubbers*, Royal Aircraft Establishment, 1967.

(6) Chinn, S.; DeTeres, S.; Sawvel, A.; Shields, A.; Balazs, B.; Maxwell, R. S. *Polym. Degrad. Stab.* 2006, *91*, 555.

(7) *Plan Information: Pressure Pads*, Kansas City Plant.

(8) Orler, E. B. *Progress Report for Post-Curing Study on the Crystallinity of DC745U*, Los Alamos National Laboratory, 2012.

(9) Iuliucci, R.; Taylor, C.; Hollis, W. K. *Magn. Reson. Chem.* **2006**, *44*, 375.

(10) Ortiz-Acosta, D.; Gallegos, J. *Low Temperature Studies on DC745U Pressure Pads*, Los Alamos National Laboratory, 2013.